ChemistrySelect

Research Article
doi.org/10.1002/slct.202200359

Chemistry Europe
European Chemical Societies Publishing

www.chemistryselect.org

Medicinal Chemistry & Drug Discovery

Pyrazolyl-Benzoxazinone Derivatives as Dual Hsp Inhibitors in Human Breast Cancer

İrfan Koca,*[a] Volkan Kamaci,[a] Ceylan Özsoy,[b] Yusuf Sert,[c] İbrahim Kani,[d, e] Lütfi Tutar,[f] and Yusuf Tutar*[g, h, i]

Heat Shock Proteins (Hsps) play major role on the onset of several cancers. Metabolic rates of cancer cells are higher compared to that of untransformed cells. This accelerated rate force functional substrate proteins to fold faster than normal folding rate. Although, the process leads cell cycle halting and eventually induces apoptosis, Hsps help cell survival and inhibit apoptosis and fold substrate proteins especially signaling proteins. When cancer cells accelerate the metabolism for invasion and metastasis, substrate proteins must fold to their native state rapidly. Since, functional forms of the proteins must be folded properly, cancer cells overexpress Hsps to fold substrate proteins and avoid apoptosis. Hsp90 and Hsp70 play key role in these processes. Inhibition of either Hsp90 or Hsp70 display complementary function. Therefore, dual inhibition of Hsp70 and Hsp90 potentially provides anticancer affect. In silico studies showed that pyrazolyl-benzoxazine derivatives display binding activity for both Hsps. For this purpose, pyrazole-3-carbonyl chloride were converted to pyrazolyl-benzoxazine derivatives via reactions of anthranilic acids in good yields (68–83 %). The structures of the newly synthesized compounds were elucidated by IR-NMR spectroscopy, elemental analysis, and single-crystal X-ray diffraction. Binding of the compounds inhibit function of Hsps and cause cytotoxic effect over MCF-7 cells. The compounds display potential anticancer effects.

Introduction

Drug design studies mimic biologically active compounds to control biochemical cascades at systemic diseases in human metabolism. However, designing site specific compounds is not an easy task. Off-target effects of designed compounds leads side effects and undesirable results. The benzoxazin-4-one template has attracted the interest of synthetic molecule designers in drug studies as benzoxazin-4-one-based compounds exhibit unique pharmacological activities. 4*H*-3,1-benzoxazin-4-ones are also important in terms of their synthesis as well as their biological effects. This scaffold is very useful precursor for the synthesis of various heterocycles, such as quinazolin-4(3*H*)-ones and 4-hydroxy-quinolin-2-(1*H*)-ones, in organic synthesis affording through reaction with nitrogen nucleophiles.[1]

The compounds are isolated from natural products, such as dianthalexin (*Dianthus caryophyllus*),[2] Avenalumins (oat leaves),[3] Cephalandoles A (*Cephalanceropsis gracilis*)[4] are 4*H*-3,1-benzoxazin-4-one derivatives (Figure 1). They own countless biological activities including anticancer,[5] anti-bacterial,[6] antifungal,[7] analgesic,[8] anti-inflammatory[9] and herbicidal activity.[10] Some of them act as inhibitors of serine proteases[11] and human leukocyte elastase.[12] Cetilistat is a drug using in the treatment of obesity. It inhibits pancreatic lipase enzyme.[13]

[a] *Prof. Dr. İ. Koca, V. Kamaci*
Faculty of Art and Science, Department of Chemistry,
Yozgat Bozok University, Yozgat, Turkey
E-mail: i_koca@yahoo.com
[b] *Prof. Dr. C. Özsoy*
Faculty of Pharmacy, Department of Basic
Pharmaceutical Sciences, Division of Biochemistry,
Cumhuriyet University, Sivas, Turkey
[c] *Prof. Dr. Y. Sert*
Sorgun Vocational School,
Yozgat Bozok University,
Yozgat, Turkey
[d] *İ. Kani*
Department of Chemistry, Faculty of Science,
Eskisehir Technical University,
Eskisehir, Turkey
[e] *İ. Kani*
Medicinal Plants and Medicine Research
Center of Anadolu University, Eskisehir, Turkey
[f] *Prof. Dr. L. Tutar*
Department of Molecular Biology and Genetics,
Faculty of Sciences, Ahi Evran University,
Kırşehir, Turkey
[g] *Y. Tutar*
Faculty of Pharmacy, Department of
Basic Pharmaceutical Sciences, D[ivision of Biochemistry,
University of Health Sciences-Turkey,
Istanbul, Turkey
E-mail: yusuf.tutar@sbu.edu.tr
[h] *Y. Tutar*
Health Sciences Institutes, Division of Oncology,
University of Health Sciences-Turkey,
Istanbul, Turkey
[i] *Y. Tutar*
Fuat Sezgin Validebağ Research Center,
University of Health Sciences-Turkey,
Istanbul, Turkey

Supporting information for this article is available on the WWW under https://doi.org/10.1002/slct.202200359

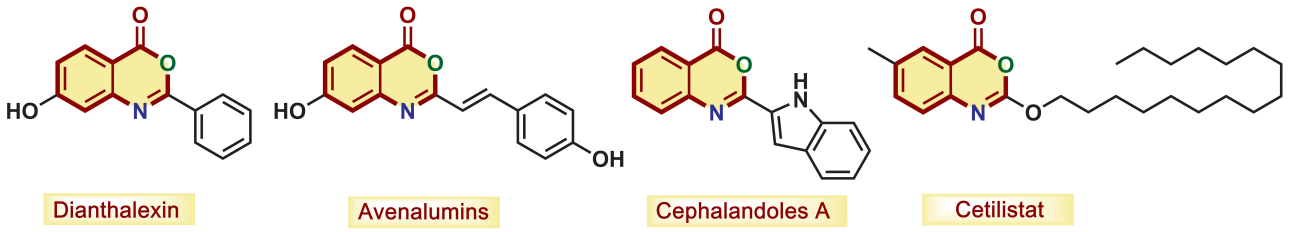

Figure 1. Some biologically important 4*H*-3,1-benzoxazin-4-one derivatives.

Pyrazole is a heterocyclic structure containing the nitrogen atom found in the structure of drugs and natural products.[14] Pyrazole derivatives as pharmaceutical agents have been used in the treatment of pain, fever, and inflammation. The derivatives have broad applications as anticancer, anti-inflammatory, antihypertensive, antidepressant, antiepileptic agents in clinic.[14c] Pyrazoles have antitumoral activity as aryl pyrazoles (Ruxolitinib and Crizotinib) (Figure 2).[14c] Both drugs are kinase inhibitor and employed in the treatment of myeloproliferative neoplasm and non-small cell lung carcinoma.[15]

In a similar fashion, pyrazole derivatives evaluated against MCF-7 human breast adenocarcinoma, NCI–H460 human non-small cell lung carcinoma, L1210 murine leukemia cell line, and SF-268 human glioblastoma cell lines displayed significant anticancer activity.[16] Cell stress exposure accumulates Hsps and Hsp90 is particularly important target in cancer pathology. Hsp90 inhibitor CCT018159 which is a pyrazole derivative reported against.[17]

In our previous study, we designed pyrazole derivative and the compounds were active against DLD-1 human colorectal adenocarcinoma, HepG2, human hepatoblastoma, and Jurkat, human T cell lymphoblast cell lines. These derivatives displayed kinase inhibition properties.[18]

Cancer is a pathological state that is a genetic and developmental process occurring due to the excessive proliferation of the cells and the loss of their apoptosis functions. In unstressed eukaryotic cells, the Hsp90 is one of the most abundant molecular chaperones that correspond to 1–2% of all cellular proteins. Hsp90 is overexpressed in tumor tissues and is required for growth and survival of cancer cells.[19]

Because of the pharmaceutical applications of both pyrazole and 4*H*-3,1-benzoxazin-4-one compounds, it is curious how benzoxazine derivatives incorporated into the pyrazole ring inhibit cancer cells. Therefore, we synthesized target compounds which could be more valuable and important pharmaceutical compounds by means of the interaction of various anthranilic acid derivatives with pyrazole-3-acid chlorides. To prevent activity of Hsps a dual inhibitor pyrazole-benzoxazin-4-ones synthesized to derive cancer cells to apoptosis for creating effective therapeutic agent. Dual Hsp90 and Hsp70 inhibition levels of the synthesized compounds were evaluated. The study aimed to inhibit overexpressed Hsps for anticancer treatment. Hsp90 inhibition induces Hsp70 expression and Hsp70 complements Hsp90 function. The effects of the compounds are promising against distinct cancer cell lines.

Results and Discussion

Chemistry

The starting materials, pyrazole-3-carbonyl chloride (**1a**,**b**), were prepared according to published methods.[20] Reaction of **1** with anthranilic acid derivatives in pyridine at 0 °C gave pyrazole-3-carboxamides (**3a-h**) in 68–83% yields (Table 1). The white-colored products **3a-h** were converted to benzoxazines (**4a-h**) with $SOCl_2$ at reflux condition. The synthesis method of

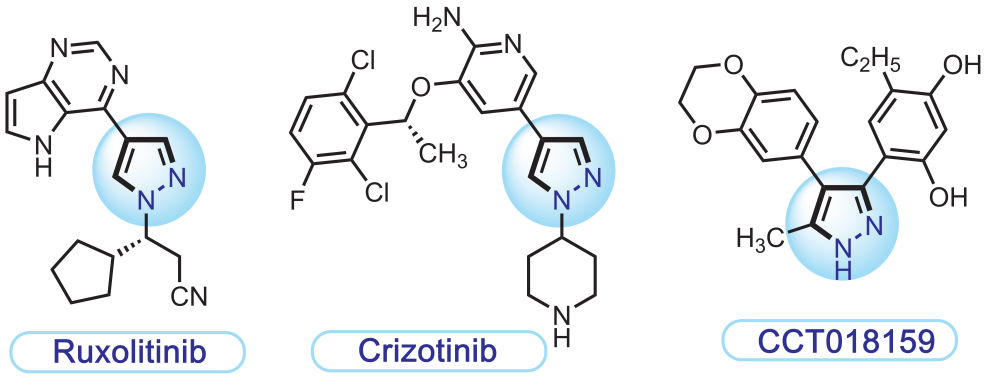

Figure 2. Some pyrazole derivative molecules with anticancer activity.

Research Article
doi.org/10.1002/slct.202200359
Chemistry Europe
European Chemical Societies Publishing

Table 1. Some properties of the target compounds **4a–h.**

Entry	Product	Mp [°C]	Mol Formula [Mol wt.]	Yields [%]	Elemental Analyses Found (Calcd) [%] C	H	N
4a	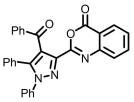	236	$C_{30}H_{19}N_3O_3$ 469.14	65	76.75 (76.65)	4.08 (3.99)	8.95 (8.60)
4b	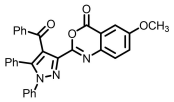	210	$C_{30}H_{19}N_3O_4$ 499.15	63	74.54 (74.14)	4.24 (4.24)	8.41 (8.15)
4c	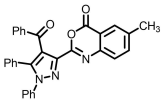	195	$C_{31}H_{21}N_3O_3$ 483.16	61	77.00 (76.76)	4.38 (4.32)	8.69 (8.41)
4d	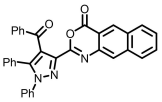	260	$C_{34}H_{21}N_3O_3$ 519.16	67	78.60 (78.52)	4.07 (3.88)	8.09 (7.82)
4e	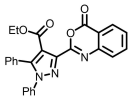	217	$C_{26}H_{19}N_3O_4$ 437.14	61	71.39 (71.28)	4.38 (4.26)	9.61 (9.42)
4f	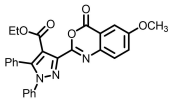	189	$C_{27}H_{21}N_3O_5$ 467.47	67	69.37 (66.29)	4.53 (4.48)	8.99 (8.85)
4g	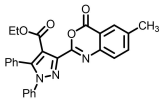	200	$C_{27}H_{21}N_3O_4$ 451.15	72	71.83 (71.68)	4.69 (4.55)	9.31 (9.26)
4h	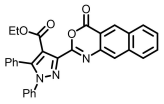	247	$C_{30}H_{21}N_3O_4$ 487.15	68	73.91 (73.88)	4.34 (4.26)	862 (8.53)

the target compounds is depicted in Scheme 1. The novel products were characterized by elemental analyses, IR, ^{1}H NMR, ^{13}C NMR and X-ray diffraction methods.The IR spectra of **3a-h** containing secondary amide group exhibit a strong absorbtion at 3282–3240 cm^{-1} which is the attributed to the N–H stretching vibration. The IR spectra of **3a-h** clearly showed absorbtion bands in the ranges of 1699–1681 (C=O, acid), 1673–1659 (C=O, amide). While compounds **3a-d** possess benzoyl group, **3e-h** possess ester group. The C=O stretch of ester group appeared at 1725–1712 cm^{-1}, while benzoyl group appeared at 1664–1655 cm^{-1}. Since the IR spectra are measured by the ATR method, characteristic broad O–H signals belonging to the acid are not fully observed. Compared to the

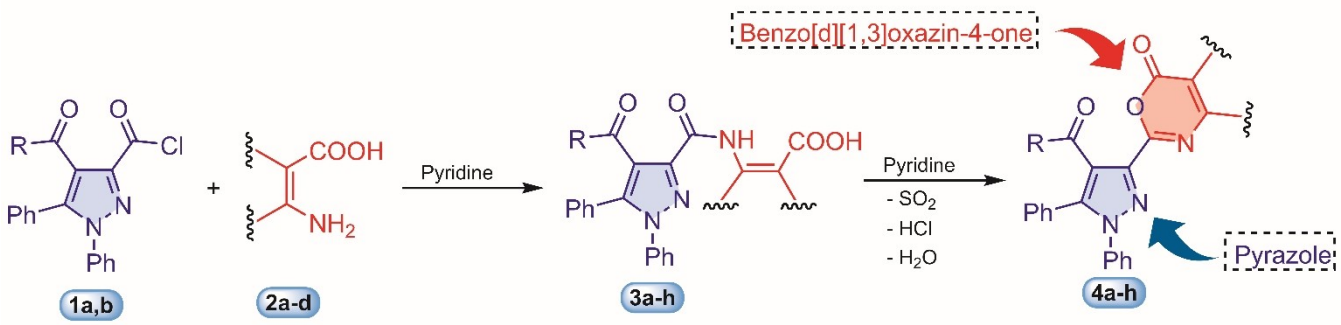

Scheme 1. The synthesis of pyrazolyl-benzoxazine derivatives **4a--h.**

IR spectra of the compounds **3** and **4**, NH bands are not seen for the compounds **4**.

The ^{1}HNMR spectrum of **3a** exhibited a broad signal belonging to the OH protons at 13.81 ppm. A singlet peak observed at 12.65 ppm is attributed to NH proton. The signals of aromatic protons of the **3a** resonated in the range of 8.52–7.14 ppm as multiplet. The ^{13}CNMR spectrum of **3a** showed three carbon signals at 191.2, 170.0, 159.2 ppm due to presence of carbonyl carbons of benzoyl, acid and amide, respectively. The signals of C=C and C=N were appeared at 144.9–116.7 ppm. When the NMR spectrum of **4a** which is cyclization product **3a** is examined, two carbonyl group signals are observed at 191.3 and 159.3 due to benzoyl and lactone group, respectively. The absorption bands were observed in the range of 1769–1750 cm^{-1} due to C=O of lactone groups for **4a-h**. Unambiguous evidence for the structure of **4a** and **4d**[21] was obtained by using X-ray analysis (Figure 3). **4a** contains heterocyclic ring structures crystallizes in monoclinic crystal system with the non centro symmetric space group P 21/c. The structure of compound **4a** has been deposited at CCDC with the deposition number CCDC 1516678. All information about experimental and theoretical studies can be found in the Supporting Information file.

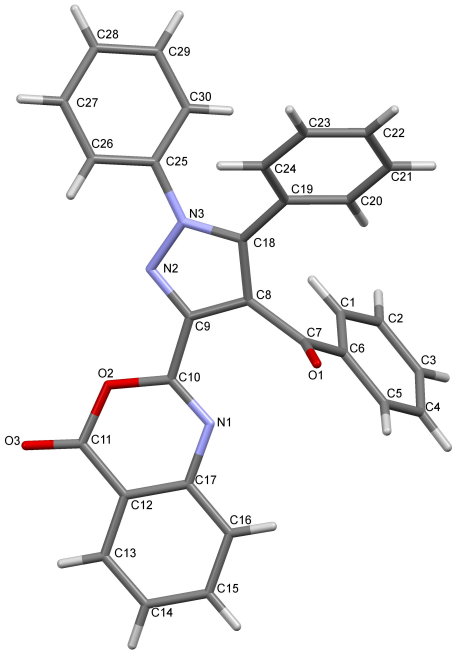

Figure 3. ORTEP Plot of **4a**, with the atom-numbering scheme.

Molecular Electrostatic Potential Analysis

Molecular electrostatic potential (MEP) is a type of analysis related to the electrostatic potential of the molecule, electronegativity and partial charges on different atoms. MEP surface analysis study, charge-dipole, dipole-dipole and it is a useful method for understanding the bonding properties of biological molecules including quadrupole-dipole interactions. The MEP map shows the shape, size, dipole moment, and relative polarity of the molecule. Electrophilic and nucleophilic reactive regions of the molecule can also be identified with the help of the MEP map. The surface map is determined by colors from red to blue, starting from the electron rich region towards the less rich regions.[22] The theoretical computations were performed Gaussian09 W package[23] and Gauss View 5.0[24] programs in this part. The MEP analysis of **4a-h** series were computed via DFT–B3LYP/6-311+G(d,p) theory-functional / basis set over the *chk files of optimized structures. The obtained MEP surfaces were shown in Figure 4.

In this study, the color scales of the **4a-h** series were determined in the range of −5.743e-2–5.543e-2 for **4a**, in the range of −5.789e-2–5.789e-2 for **4b**, in the range of −6.126e-2–6.126e-2 for **4c**, inthe range of −5.876e-2–5.876e-2 for **4d**, in the range of −5.727e–5.727e-2 for **4e**, in the range of −5.775e-

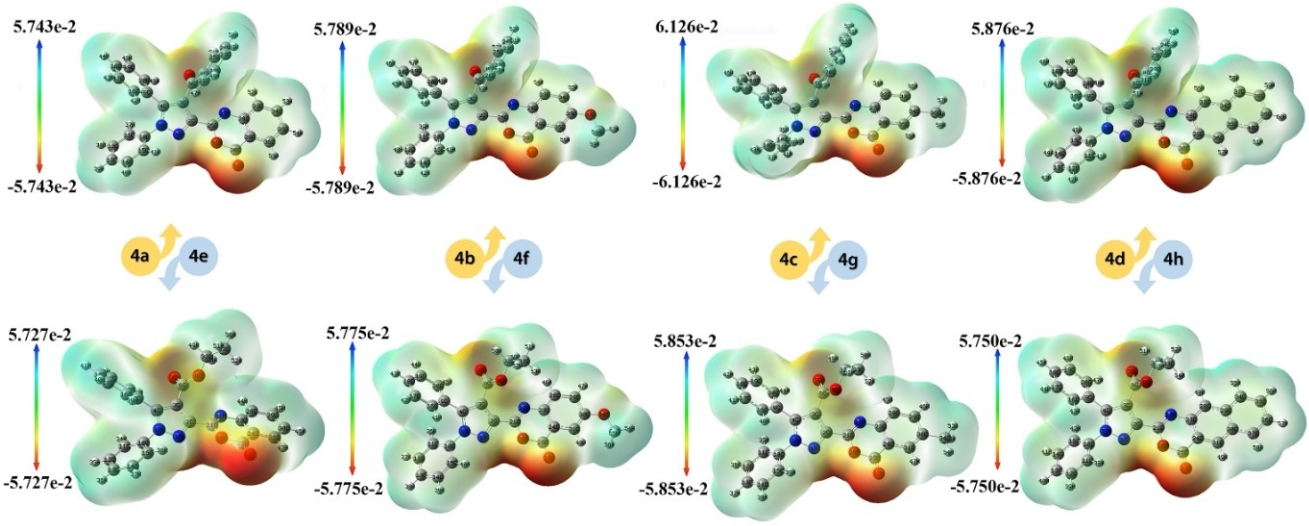

Figure 4. The MEP surfaces of synthesized **4a–h** series.

2–5.775e-2 for **4f**, in the range of −5.853e-2–5.853e-2 for **4g** and in the range of −5.750e-2–5.750e-2 for **4h**. From the results, dark red or negative points were concentrated on the oxygen atoms of the benzoxazine group (O26, O27, O30, O31, O32 according to the numbering format in Figure 4) and partially on O7 atoms of all series, these points indicate most electron-rich regions or nucleophilic. On the other hand, in regions around the rest of the molecule with green colour, electron density was found to be less. The green parts indicate that the C–H hydrogens are in the electrophilic region. According to this result, O atoms undergo electrophilic reaction and these

Molecular docking analysis

The binding interactions of drugs with the target macromolecule are mostly through intermolecular bonds. Besides electrostatic bonds, the most common bonds are hydrogen bonds and Van der Waals' interactions. In the optimization of lead compounds with potential to be drug candidates, considering these interactions, various substituents are connected and their effects on activity and selectivity are investigated. Possible effects can be investigated by studies such as structure-activity relationships, molecular docking, and pharmacophore in the computer database. In this context, molecular docking or in silico computations is indispensable in pharmaceutical chemistry for preliminary evaluations.[25] In this part, in silico-molecular docking studies of benzoxazine derivatives such as **4a–h** considered as dual HSP inhibitors with HSP70/PDB:1S3X and HSP90/PDB:1YC4 receptors were performed by AutoDock Vina program.[26] The related receptors were obtained from RCSB (Protein Data Bank).[27] The preparations such as the removing of hetero groups and the addition of polar hydrogen bonds for both the receptors and ligands and in docking were made via Discover Studio Visualizer 4.0 (DSV 4.0) software.[27b] Firstly, the active sites of the HSP70/PDB:1S3X and HSP90/PDB:1YC4 receptors were determined, respectively as: ASP366, ARG342, SER340, GLY339, GLY338, SER275, ARG272, LYS271, GLU268, ASP232, GLU231, GLY230, HIS227, ASP206, THR204, GLY202, GLY201, ASP199, GLU175, PRO147, LYS71, THR15, THR14, THR13, GLY12, ASP10 for HSP70/PDB:1S3X and VAL186, THR184, PHE138, MET98, GLY97, ILE96, ASP93, LYS58, ALA55, ASN51 for HSP90/PDB:1YC4. The grid parameters determined according to the active sites of both receptors can be given as follows: 110x108x82 Å3 x,y,z dimesions, 0.375 Å space and 17.349, 28.677, 15.278 x,y,z centers for HSP70/PDB:1S3X and 50x50x54 Å3 x,y,z dimesions, 0.375 Å space and 34.008, 31.908, −4.657 x,y,z centers for HSP90/PDB:1YC4. Additionally, as ligands were used the optimized structures (at B3LYP/6-311G (d, p) fuctional/basis level) of benzoxazine derivatives (**4a–h**). The obtained molecular docking binding energy values and Ki values accordingly obtained were presented in Table 2. Furthermore, the molecular docking interaction situations for **4a–h** + HSP70/PDB:1S3X and **4a–h** + HSP90/PDB:1YC4 were given in Supplementary Information. As can be seen from the docking results between ligands and dual HSP receptors in Table 2, although **4a–h** ligands have the potential to inhibit both receptors (HSP70/PDB:1S3X and HSP90/PDB:1YC4), it is noticed that the results obtained for HSP70 are more dominant in terms of binding energies and Ki values. The Ki values were obtained with exp(ΔG/RT) equation. Here, ΔG is binding energy, R is gas constant = 1.9872036×10^{-3} kcal/mol and T is room temperature = 298.15 K.

Table 2. Molecular docking scores of **4a–h** series.

COMPOUNDS	HSP70/PDB: 1S3X Binding Energy (kcal/mol)	Ki values (μm)
4a	−9.30	0.152423
4b	−11.20	0.00617078
4c	−10.90	0.0102386
4d	−10.80	0.0121211
4e	−9.60	0.0918647
4f	−9.80	0.0655462
4g	−10.00	0.0467678
4h	−8.20	0.97579
COMPOUNDS	HSP90/PDB:1YC4 Binding Energy (kcal/mol)	Ki values (μm)
4a	−9.10	0.213625
4b	−8.70	0.419618
4c	−7.80	1.91672
4d	−10.10	0.0395045
4e	−8.80	0.354448
4f	−7.10	6.24687
4g	−8.60	0.496769
4h	−9.30	0.152423

The obtained results could be evaluated as follows: the best binding or the smallest Ki value was obtained between **4b** and HSP70/PDB: 1S3X with 11.20 kcal/mol energy and 0.00617078 μm Ki value. When all the energy values were listed, it was observed that **4b** > **4c** > **4d** > **4g** > **4f** > **4e** > **4a** > **4h**. When the obtained for the best binding (**4b** + HSP70/PDB:1S3X) in Figure 5 was examined, van der Waals, carbon-hydrogen bond, π-cation, π-anion, π-donor hydrogen bond and π-alkyl interactions were

determined. In addition, the position of the best poses of the **4b** molecule in the active site of the HSP70/PDB: 1S3X could be seen as in Figure 5.

Secondly, the best binding value was obtained between **4d** and HSP90/PDB: 1YC4 with 10.10 kcal/mol energy and 0.0395045 μm Ki value. When all the energy values were listed, it was observed that **4d** > **4h** > **4a** > **4e** > **4b** > **4g** > **4c** > **4f**. When the obtained for the best binding (**4d** + HSP70/PDB:1S3X) in Figure 5 was evaluated, van der Waals, π-cation, π-anion, π-donor hydrogen bond, amide-π-stacked and π-alkyl interactions were observed. Additionally, the position of the best poses of the **4d** molecule in the active site of the HSP90/PDB: 1YC4 could be observed as in Figure 5.

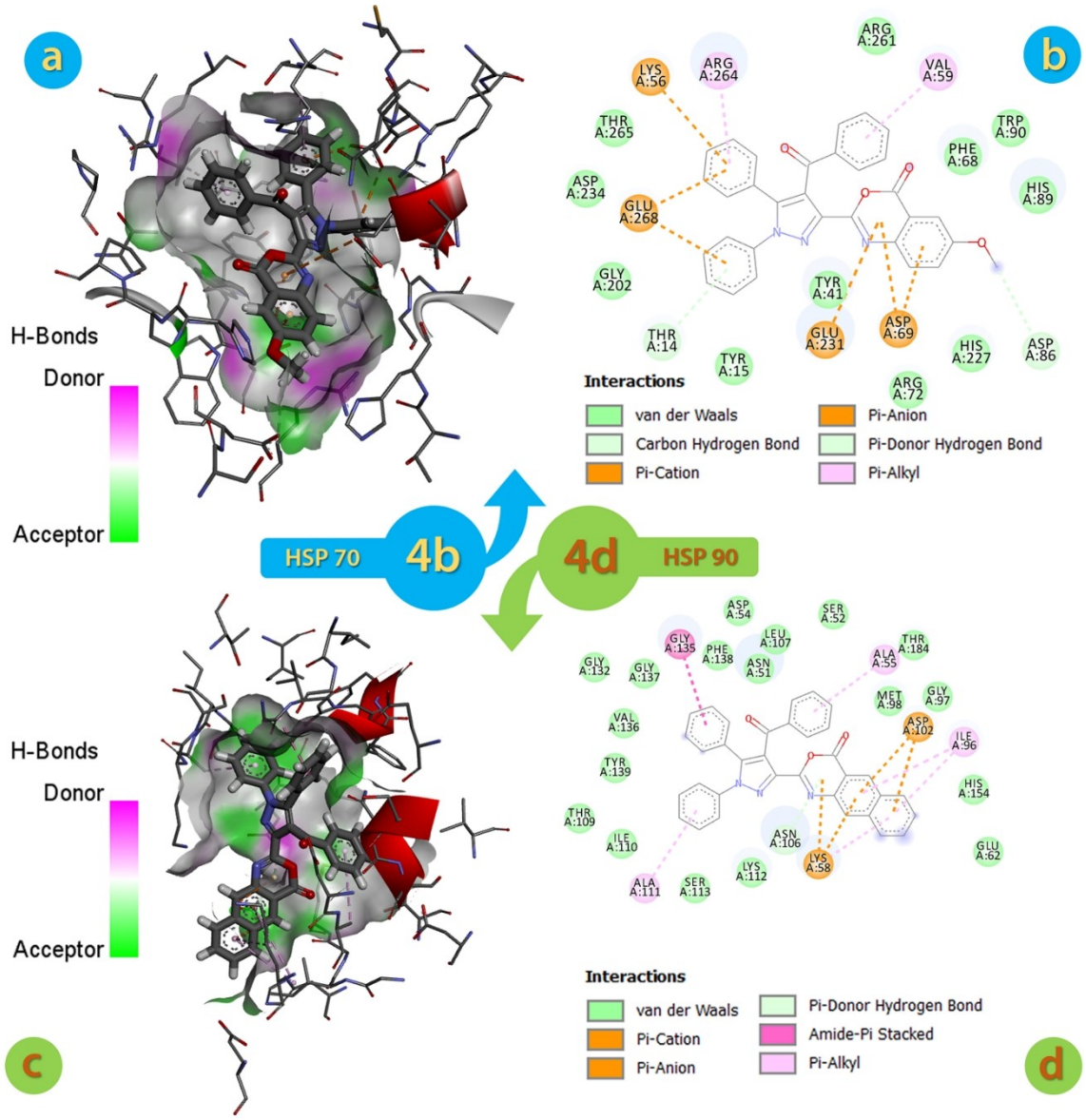

Figure 5. (a) 3D and (b) 2D molecular docking results of the **4b** + HSP70/PDB: 1S3X. (c) 3D and (d) 2D molecular docking results of the **4d** + HSP90/PDB: 1YC4.

Drug-Likeness and ADMET Studies

The most effective and quickest method for determining drug-like properties of a molecule is to check whether it complies with Lipinski rules (RO5), and these rules are very curucial for oral usage.[28] According to these five rules:

- *n*-octanol/water partition coefficient (MlogP) ≤ 5
- Molecular weight (MW) ≤ 500 g/mol
- Number of H-bond acceptor (HBA) ≤ 10; number of H-bond donors (HBD) ≤ 5
- Number of rotatable bonds (nRot) ≤ 10
- Topological Polar Surface Area (TPSA) < 140 Å^2

In this research, these drug-likeness rules for our **4a–h** series were examined from physicochemical properties section of SwissADME web page[29] and listed as in Table 3. According to the results, while one violations were observed in the **4d** molecule (MW > 500), no violations were found for the other molecules.

The molar refractivity (MR) values, which are other physicochemical properties were determined as 138.15, 144.64, 142.11, 155.65, 124.36, 130.85, 129.33, 141.87. In addition, log S (Ali: aqueous solubility) values, which are property of water solubility were computed as −7.65, −7.82, −7.99, −8.95, −6.69, −6.85, −7.07, −7.98 for **4a–h** series, respectively. Finally, inhibitor (+) and non-inhibitor (−) characteristic of CYP450 enzymes like CYP1A2, CYP2C19, CYP2C9, CYP2D6 and CYP3A4 were researched. As seen from the Table 3, the inhibitory effect was not observed in all molecules (**4a–h** series) for CYP1A2 and CYP2D6 enzymes. Later, it was determined that the **4c** molecule had inhibition properties against CYP2C19 and the **4f**

Table 3. Important computed physicochemical properties of the **4a-h** series.

Compound	**4a**	**4b**	**4c**	**4d**	**4e**	**4f**	**4g**	**4h**
MW	469.49	499.52	473.52	519.55	437.45	467.47	451.47	487.51
n_{Rot}	5	6	6	5	6	7	6	6
HBA	5	6	5	5	6	7	6	6
HBD	0	0	0	0	0	0	0	0
Mlog *P*	3.94	3.33	3.73	4.52	3.36	3.04	3.56	3.98
TPSA	77.99	87.22	77.99	77.99	87.22	96.45	87.22	87.22
log *S* (Ali)	−7.65	−7.82	−7.99	−8.95	−6.69	−6.85	−7.07	−7.98
MR	138.15	144.64	142.11	155.65	124.36	130.85	129.33	141.87
CYP1A2 inhibitor	−	−	−	−	−	−	−	−
CYP2C19 inhibitor	−	−	+	−	−	−	−	−
CYP2C9 inhibitor	−	+	+	−	+	+	+	+
CYP2D6 inhibitor	−	−	−	−	−	−	−	−
CYP3A4 inhibitor	−	−	−	−	−	+	−	−
Lipinski rule violation	0	0	0	1	0	0	0	0

molecule against CYP3A4 enzymes. In addition, it was observed that molecules **4b**, **4c**, **4e**, **4f**, **4g** and **4h** were able to inhibit the CYP2C9 enzyme. Finally, bioavailability radars (according to Lipinski rules) and predicted boiled-egg plots (BBB relation) of **4a**–**h** molecules were obtained and depicted as Figure 6 and 7, respectively.

ADMET (Absorption, Distribution, Metabolism, Excretion and Toxicity) properties are very curucial in-silico and in-vitro drug screening for pharmacology. Because, drug-likeness candidates should over run the ADMET required. In this step of research, the some important ADMET features of **4a**–**h** series were obtained with the help of AdmetSAR 2.0[30] over the output forms and the obtained scores were presented in Table 4. Now, let's look at the absorption properties of Blood brain barrier (BBB), Human intestinal absorption value and P-glycoprotein inhibitor. BBB values were found positive for our series and the values were acquired in the range of 0.8447 (**4f**)-0.9781 (**4a** and **4d**). The closeness of these values to BBB could be easily seen from Figure 7. The second parameter for absorption is human intestinal absorption. These parameters were found as positive in the range of 0.9945 (for **4b**)-1.0000 (for **4c**, **4e** and **4h**). As the third, P-glycoprotein inhibitor

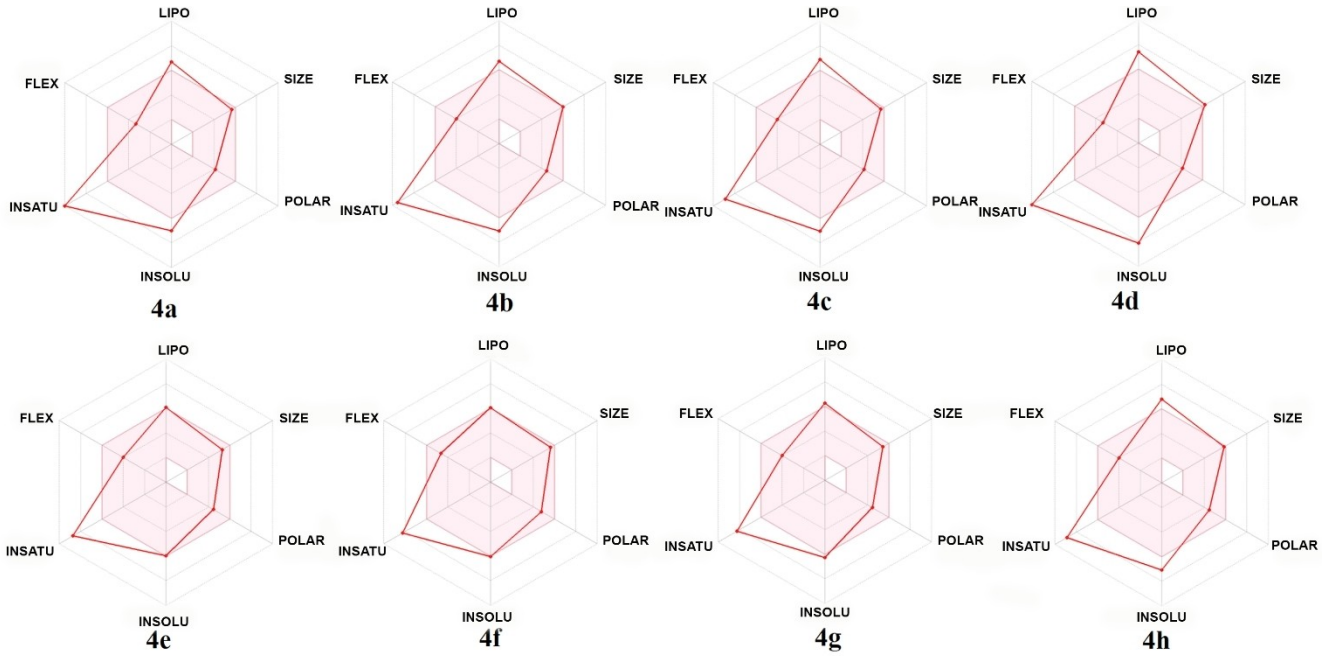

Figure 6. The bioavailability radars of **4a**–**h** series.

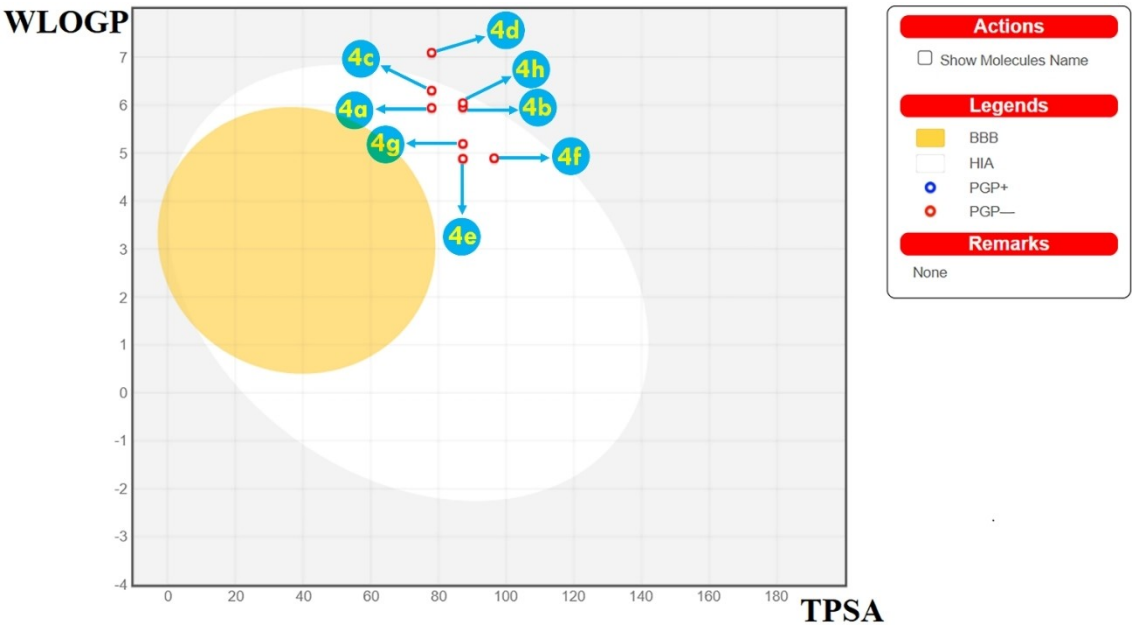

Figure 7. The boiled-egg plots of the **4a–h** series.

Table 4. Selected pharmacokinetic parameters of **4a-h** series.

Compound	Blood brain barrier	Human intestinal absorption	P-glycoprotein inhibitor	hERG	Carcinogen	Acute oral toxicity
4a	+(0.9781)	+(0.9973)	NI(0.6566)	WI(0.9688)	NC(0.8903)	III(0.7337)
4b	+(0.8913)	+(0.9945)	I(0.5707)	WI(0.9727)	NC(0.9001)	III(0.7109)
4c	+(0.8746)	+(1.0000)	NI(0.8376)	WI(0.9588)	NC(0.8854)	III(0.6931)
4d	+(0.9781)	+(0.9973)	NI(0.6566)	WI(0.9688)	NC(0.8903)	III(0.7337)
4e	+(0.9175)	+(1.0000)	NI(0.7166)	WI(0.9786)	NC(0.8530)	III(0.7815)
4f	+(0.8447)	+(0.9956)	I(0.5881)	WI(0.9784)	NC(0.8637)	III(0.7484)
4g	+(0.8931)	+(0.9967)	NI(0.6461)	WI(0.9841)	NC(0.8300)	III(0.7649)
4h	+(0.9175)	+(1.0000)	NI(0.7166)	WI(0.9786)	NC(0.8530)	III(0.7815)

I: Inhibitor; NI: Non Inhibitor; WI: Weak Inhibitor; NC: Non-Carcinogens

situations were researched and it is found that **4a-h** series show non-inhibitor properties generally, but for **4b** and **4f** molecules indicate the inhibitory effect. The founded values for P-glycoprotein inhibitor were determined range from 0.5707 (**4b** inhibitor effect) to 0.8376 (**4c** non-inhibitor effect). Finally, when we look at toxicity features such as hERG, Carcinogen, Acute oral toxicity; we can observed that **4a–h** series indicate the weak inhibitor property against hERG-human ether-a-go-go-related gene, and these values were found between 0.9588 (**4c**) and 0.9841 (**4g**). When the other two parameters (carcinogen and acute oral toxicity) were evaluated, it was observed that the whole series were non-carcinogen and the acute oral toxicity values were in class III.

Anticancer activity of new pyrazole-benzoxazine derivatives

In this study, the anticancer activity of eight pyrazole-benzoxazine derivatives was tested in vitro against the ER+ breast cancer cell line MCF-7. Four different concentrations (12.5, 25, 50, 100 μM) of target compounds were applied to the cells. After 24 and 48 hours, cell viability was determined with the XTT test protocol and the results were compared with control cells (untreated cells) to determine anticancer properties. (Table 5).

Cell cytotoxicity experiments displayed promising results. Structure of pyrazolyl-benzoxazinone derivatives have adverse results on cell line. The toxicity of each compound further enhances with daily treatment. **4a**, **4b**, **4c**, **4h** effectively inhibit

Table 5. IC_{50} values of Benzoxazines derivatives.

Compounds	IC50/μM (24 h)	(48 h)
4a	20	41
4b	24	21
4c	19	20
4d	46	20
4e	42	62
4f	36	22
4g	48	23
4h	23	60

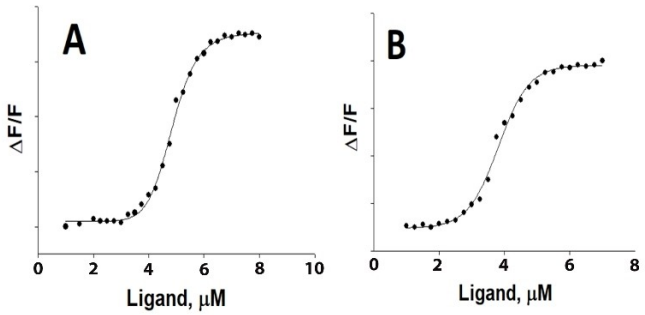

Figure 8. Ligand **4b** binding to full length Hsp70 (A) and Hsp90α (B) by fluorometric titration experiments.

cancer cells at 24 hours but **4a** and **4h** decrease their activity at 48 hours. Similarly, **4d**, **4f**, **4g** exert their optimal activity at 48 hours. Further, **4b** and **4c** display similar activity both at 24 and 48 hours (Table 5). *In silico* assay indicate that each derivative has similar binding energy with distinct inhibition constant. However, **4a**, **4e** and **4h** display higher inhibition and IC_{50} values. Thus, inhibitor structure has minimal effect on Hsp binding but variable effect on Hsp conformation. As a result, conformational changes upon inhibitor binding determines degree of cell cytotoxicity. This effect is most probably originating from cochaperone binding efficiency of Hsp structures. It should be noted that in vitro protein binding concentration is lower that of *in silico* because conformational changes can be tracked by fluorescence binding experiments readily. Therefore, inhibitor binding to Hsp structures determines degree of cell cytotoxicity. In this sense, pyrazolyl-benzoxazinone derivatives provide unique template for Hsp inhibition and clinical drug design.

Fluorescence Binding Studies

Full length Hsp70 and Hsp90α bind **4b** efficiently with 4.91 and 4.01 μM respectively. The values are slightly different than that of in silico experiments. Since these proteins are in intact form, compact structures may bind tightly (Figure 8).

The compound binds both Hsp70 and Hsp90 and may act as dual inhibitor. The results correlate with cell cytotoxicity experiments.

Conclusion

The novel pyrazole-benzoxazine hybrid molecules were synthesized and investigated for their potential anticancer activities by XTT cell proliferation assay. And also, fluorescence binding experiments of **4b** were done. The obtained data showed that the compound binds both Hsp70 and Hsp90 and may act as dual inhibitor. Moreover, in silico-molecular docking calculations of the **4a**–**h** series, which are considered to be dual HSP inhibitors (HSP70/PDB:1S3X and HSP90/PDB:1YC4) were made with great care by taking into account the validation rules and evaluating binding active pockets (the most potent) with Autodock Vina program. As mentioned above, it was noticed that the binding values for both targets were quite good and the series showed promise as a dual HSP inhibitor. The results are supported by fluorescence binding experiments. Finally, it can be said that the **4a**–**h** series exhibit good pharmacokinetic properties due to drug-likeness and some important ADMET properties. As can be seen, the theoretical calculations of the synthesized compounds ADMET results are in agreement with Lipinski's five rule. Considering the results obtained, it can shed light on future experimental researches and drug candidates.

Supporting Information Summary

The Supporting Information file includes general experimental section, general methods of synthesis and spectral data as well as spectral copy of the synthesized compounds. Moreover, The methods used for biological testing, and docking procedures were explained in this section.

Author Contributions

All authors have made essential contributions to this study. Establishing the outline of the study: İK, YT; Synthesis and characterization: VK, İK; Crystallography: İb.K.; Molecular Docking studies: YS; Biological activity studies: CÖ, LT, YT; Manuscript drafting; İK, YS, YT. All authors read and approved the final manuscript.

Acknowledgements

Synthesis studies were carried out within the scope of Volkan Kamacı's master's thesis studies.[31] For characterization, relevant corresponding spectra (IR, NMR) can be found in the related thesis. This work was funded through a seed grand from Science and Technology Practice & Research Centre of Yozgat Bozok University (Project No: 2015 FBE/T167) and Turkish National Academy of Sciences for YT. The authors gratefully acknowledge the Medicinal Plants and Medicine Research Centre of Anadolu University, Eskişehir, Turkey, for the use of X-ray Diffractometer.

Conflict of Interest

The authors declare that they have no known competing financial interests or personal relationships that could have appeared to influence the work reported in this paper.

Data Availability Statement

The data that support the findings of this study are available from the corresponding author upon reasonable request.

Keywords: Benzoxazine · Breast Cancer · HSP · Molecular Docking · Pyrazole

[1] a) M. S. Mohamed, M. M. Kamel, E. M. Kassem, N. Abotaleb, S. I. Abd El-moez, M. F. Ahmed, *Eur. J. Med. Chem.* **2010**, *45*, 3311–3319; b) A. Mrozek-Wilczkiewicz, D. S. Kalinowski, R. Musiol, J. Finster, A. Szurko, K. Serafin, M. Knas, S. K. Kamalapuram, Z. Kovacevic, J. Jampilek, *Bioorg.*

Med. Chem. **2010**, *18*, 2664–2671; c) C. A. Mosley, T. M. Acker, K. B. Hansen, P. Mullasseril, K. T. Andersen, P. Le, K. M. Vellano, H. Bräuner-Osborne, D. C. Liotta, S. F. Traynelis, *J. Med. Chem.* **2010**, *53*, 5476–5490; d) A. Detsi, V. Bardakos, J. Markopoulos, O. Igglessi-Markopoulou, *J. Chem. Soc., Perkin Trans. 1* **1996**, 2909–2913; e) C. Mitsos, A. Zografos, O. Igglessi-Markopoulou, *Org. Lett* . **1999**,1953–1955 .

[2] M.-L. Bouillant, J. Favre-Bonvin, P. Ricci, *Tetrahedron Lett.* **1983**, *24*, 51–52.

[3] S. Mayama, *The role of avenalumin in the resistance of oats to crown rust.* **1983**, *42*, 64.

[4] J. J. Mason, J. Bergman, T. Janosik, *J. Nat. Prod.* **2008**, *71*, 1447–1450.

[5] T. M. Abdel-Rahman, *J. Heterocycl. Chem.* **2005**, *42*, 1257–1265.

[6] E. Tanta, *Acta Pharm* **2000**, *50*, 239–248.

[7] a) M. Hauteville, M. Ponchet, P. Ricci, J. Favre-Bonvin, *J. Heterocycl. Chem.* **1988**, *25*, 715–718; b) A. A. Shalaby, A. M. A. El-Khamry, S. Shiba, A. A. A. E. A. Ahmed, A. A. Hanafi, *Arch. Pharm.* **2000**, *333*, 365–372.

[8] Z. A. Khan, S. A. R. Naqvi, S. A. Shahzad, N. Mahmood, M. Yar, A. F. Zahoor, *Asian J. Chem.* **2013**, *25*, 152–156.

[9] S. K. Rao, L. V. Narayana, P. K. Dube, V. Aparna, *Heterocycl. Commun.* **2003**, *9*, 51–56.

[10] Z. Hussain, Z. A. Khan, *J. Chem. Soc. Pak.* **2013**, *35*, 450–456.

[11] S. J. Hays, B. W. Caprathe, J. L. Gilmore, N. Amin, M. R. Emmerling, W. Michael, R. Nadimpalli, R. Nath, K. J. Raser, D. Stafford, *J. Med. Chem.* **1998**, *41*, 1060–1067.

[12] A. Krantz, R. W. Spencer, T. F. Tam, T. J. Liak, L. J. Copp, E. M. Thomas, S. P. Rafferty, *J. Med. Chem.* **1990**, *33*, 464–479.

[13] V. Hainer, *Expert Opin. Pharmacother.* **2014**, *15*, 1975–1978.

[14] a) A. Ansari, A. Ali, M. Asif, Shamsuzzaman, *New J. Chem.* **2017**, *41*, 16–41; b) P. Moreau, F. Anizon, F. Giraud, Y. J. Esvan, *Recent Pat. Anti-Cancer Drug Discovery* **2016**, *11*, 309–321; c) Ş. G. Küçükgüzel, S. Şenkardeş, *Eur. J. Med. Chem.* **2015**, *97*, 786–815.

[15] R. Perez-Fernandez, P. Goya, J. Elguero, *ARKIVOC* **2014**, (ii) 233–293.

[16] a) P. G. Baraldi, I. Beria, P. Cozzi, C. Geroni, A. Espinosa, M. A. Gallo, A. Entrena, J. P. Bingham, J. A. Hartley, R. Romagnoli, *Bioorg. Med. Chem.* **2004**, *12*, 3911–3921; b) A. H. Abadi, A. A. H. Eissa, G. S. Hassan, *Chem. Pharm. Bull.* **2003**, *51*, 838–844.

[17] K.-M. J. Cheung, T. P. Matthews, K. James, M. G. Rowlands, K. J. Boxall, S. Y. Sharp, A. Maloney, S. M. Roe, C. Prodromou, L. H. Pearl, *Bioorg. Med. Chem. Lett.* **2005**, *15*, 3338–3343.

[18] a) İ. Koca, A. Özgür, K. A. Coşkun, Y. Tutar, *Bioorg. Med. Chem.* **2013**, *21*, 3859–3865; b) K. A. Coşkun, İ. Koca, M. Gümüş, Y. Tutar, *Anti-Cancer Agents Med. Chem.* **2021**, *21*, 1472–1480.

[19] M. Shevtsov, G. Multhoff, *Front. Immunol.* **2016**, *7*, 171.

[20] a) Y. Akçamur, G. Penn, E. Ziegler, H. Sterk, G. Kollenz, K. Peters, E. Peters, H. Von Schnering, *Monatsh. Chem* **1986**, *117*, 231–245; b) A. Şener, İ. Bildirici, İ. Tozlu, H. Genç, K. Arısoy, *J. Heterocycl. Chem.* **2007**, *44*, 1077–1081.

[21] Y. Sert, M. Gümüş, V. Kamaci, H. Gökce, İ. Kani, İ. Koca, *J. Theor. Comput. Chem.* **2017**, *16*, 1750039.

[22] P. Politzer, J. S. Murray, *Molecular Electrostatic Potentials*, Taylor & Francis Group, LLC: New York, **2004**.

[23] M. Frisch, G. Trucks, H. B. Schlegel, G. E. Scuseria, M. A. Robb, J. R. Cheeseman, G. Scalmani, V. Barone, B. Mennucci, G. Petersson, *Gaussian 09; Gaussian, Inc., Wallingford CT* **2009**, *201*.

[24] R. Dennington, T. Keith, J. Millam, *Received: May* **2013**, *23*.

[25] S. F. Sousa, P. A. Fernandes, M. J. Ramos, *Proteins: Struct., Funct., Bioinf.* **2006**, *65*, 15–26.

[26] O. Trott, A. J. Olson, *J. Comput. Chem.* **2010**, *31*, 455–461.

[27] a) https://www.rcsb.org/; b) https://www.3dsbiovia.com/; c) A. Kreusch, S. Han, A. Brinker, V. Zhou, H.-s. Choi, Y. He, S. A. Lesley, J. Caldwell, X.-j. Gu, *Bioorg. Med. Chem. Lett.* **2005**, *15*, 1475–1478; d) M. Sriram, J. Osipiuk, B. Freeman, R. Morimoto, A. Joachimiak, *Structure* **1997**, *5*, 403–414.

[28] C. A. Lipinski, F. Lombardo, B. W. Dominy, P. J. Feeney, *Advanced drug delivery reviews* **1997**, *23*, 3–25.

[29] Swiss Instute of Bioinformatics to be found under http://www.swissadme.ch/.

[30] https://academic.oup.com/bioinformatics/article/35/6/1067/5085368.

[31] V. Kamacı, The Synthesis Studies of Novel Compounds From Pyrazole Compounds, Master of Science Thesis, Bozok University **2016**.

Submitted: January 27, 2022
Accepted: May 4, 2022